# Noise Studies of Externally Dispersed Interferometry for Doppler Velocimetry

David J. Erskine[a], Jerry Edelstein[b], James P. Lloyd[c], and Philip S. Muirhead[c]

[a]Lawrence Livermore Nat. Lab., 7000 East Ave, Livermore, CA 94550
[b]Space Sciences Lab. at Univ. of Calif., Berkeley, CA 94720-7450
[c]Astronomy Dept., Cornell University, Ithaca, NY 14853

## ABSTRACT

Externally Dispersed Interferometry (EDI) is the series combination of a fixed-delay field-widened Michelson interferometer with a dispersive spectrograph. This combination boosts the spectrograph performance for both Doppler velocimetry and high resolution spectroscopy. The interferometer creates a periodic comb that multiplies against the input spectrum to create moiré fringes, which are recorded in combination with the regular spectrum. Both regular and high-frequency spectral components can be recovered from the data– the moiré component carries additional information that increases the signal to noise for velocimetry and spectroscopy. Here we present simulations and theoretical studies of the photon limited Doppler velocity noise in an EDI. We used a model spectrum of a 1600K temperature star. For several rotational blurring velocities 0, 7.5, 15 and 25 km/s we calculated the dimensionless Doppler quality index ($Q$) versus wavenumber $\nu$. This is the normalized RMS of the derivative of the spectrum and is proportional to the photon-limited Doppler signal to noise ratio.

**Keywords:** Doppler planet search, radial velocity, interferometry, high resolution spectroscopy

## 1. INTRODUCTION

There has been interest in a new technique called Externally Dispersed Interferometry[1–14] for boosting the performance of spectrographs for Doppler velocimetry and high resolution spectroscopy. In EDI a comparatively small fixed-delay field-widened Michelson interferometer is added in series with a dispersive spectrograph (Fig. 1). The interferometer creates a periodic transmission comb that multiplies against the input spectrum to create moiré fringes, which are recorded in combination with the regular spectrum. A Doppler velocity change induces a phase change in the moiré pattern relative to the moiré pattern of a calibrant spectrum measured simultaneously. The moiré pattern has much broader features than the narrow stellar absorption lines that created it. Hence a much lower resolution spectrograph can be used to make precision Doppler velocities than otherwise practical without the interferometer. In fact the native spectrograph can have a low resolution (3k to 6k) such that the stellar lines are not fully resolved. Such an EDI has been used to discover a new exoplanet recently.[14]

We plan[12] to field an EDI at the Mt. Palomar Observatory 200 inch telescope in series with the 3k resolving power TripleSpec near infrared spectrograph[15] being built by Cornell University. The objects of interest are exoplanets around cool stars.

We present simulations and theoretical studies of the photon limited Doppler velocity noise in an EDI. Here we used a model spectrum[16] of a 1600K temperature star calculated to high resolution by Didier Saumon, Mark Marley and Richard Freeman. For several rotational blurring velocities 0, 7.5, 15 and 25 km/s we calculated the dimensionless Doppler quality index ($Q$) versus wavenumber $\nu$. This is the normalized RMS of the derivative of the spectrum. The photon limited Doppler noise ($\delta V$) is inversely proportional to $Q$, so a high $Q$ is desired to produce a large signal to noise ratio. Figure 7 is an example result for $Q$ vs wavenumber, discussed in more detail later.

Further information: http://www.spectralfringe.org/EDI
D.E.: erskine1@llnl.gov, 925-422-9545; J.E.: jerrye@ssl.berkeley.edu, 510-642-0599
J.L.: jpl@astro.cornell.edu, 607-255-4083; P.M.: muirhead@astro.cornell.edu, 607-255-6307

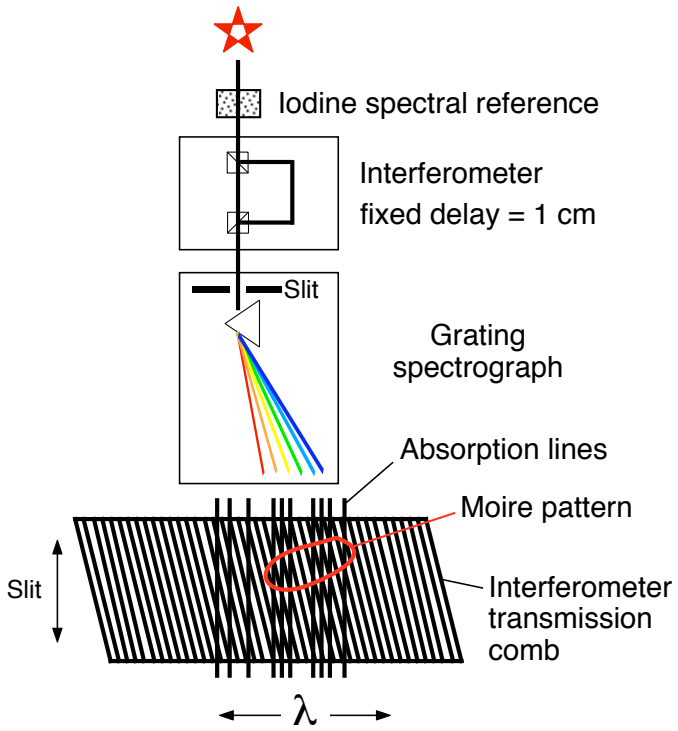


**Figure 1.** Principle of EDI: a white-light, unequal-arm interferometer feeds a spectrograph and produces spectral fringes that beat with the source's spectrum and create a recordable moiré pattern. The overall phase of the stellar moiré pattern relative to the moiré pattern of an iodine spectral reference shifts proportional to the stellar Doppler velocity. The advantage of the EDI is that an inexpensive and high throughput low resolution spectrograph can be used to measure precision Doppler velocities, previously requiring a high resolution spectrograph.

## 2. INSTRUMENT THEORY

### 2.1. Conventional spectrograph theory

Wavenumber $\nu = 1/\lambda$ is the preferred dispersion variable rather than wavelength $\lambda$ since the interferometer sinusoidal comb is periodic in $\nu$.

The conventional (purely dispersive spectroscopy) detected signal versus wavenumber, $S_c(\nu)$, is the convolution of the intrinsic input spectrum, $S_0(\nu)$, and the native spectrograph line spread function $LSF_0(\nu)$,

$$S_c(\nu) = S_0(\nu) \otimes LSF_0(\nu) \ . \tag{1}$$

The convolution of Eq. 1 is conveniently expressed in Fourier-space as a product,

$$s_c(\rho) = s_0(\rho) \ lsf_0(\rho), \tag{2}$$

where lower case symbols represent the Fourier transforms, and $\rho$ is the feature frequency along the dispersion axis in features per cm$^{-1}$, which also has units of cm. The $lsf(\rho)$ is thus the instrument modulation transfer function, and is the Fourier transform of the impulse response $LSF(\nu)$.

### 2.2. EDI theory

The normalized interferometer transmission $T(\nu)$ is a sinusoidal spectral comb,

$$T(\nu) = 1 + \gamma \cos(2\pi\tau\nu + \phi) \ , \tag{3}$$

where $\gamma$ is the interferometer visibility, assumed unity for now, and $\tau$ is the interferometer delay (optical pathlength difference between its two arms) in units of cm. By moving an interferometer mirror mounted on a PZT transducer slight delay changes can be made which are equivalent to phase changes $\Delta\phi = 2\pi\Delta\tau/\lambda$.

Raw fringing spectra $B_\phi$ are recorded at multiple phase values $\phi$, such as differing by $\sim 90°$, designated $B_0$, $B_{90}$, etc. The passage of light through the interferometer multiplies the spectral comb $T(\nu)$ with the spectrum prior to blurring by the external spectrograph. Hence the EDI detected signal is

$$B_\phi(\nu) = [S_0(\nu)\ T(\nu)] \otimes LSF_0(\nu)\ . \tag{4}$$

The EDI fringing spectrum is obtained by summing the exposures after numerically rotating them by $\theta$ so that the hardware applied phase steps $\phi$ are reversed and add sympathetically. The fringing spectrum is called a "whirl", represented by symbol $\mathbf{W}(\nu)$, and is complex, where the complex magnitude and phase represent the fringe phase and magnitude for that wavenumber channel. The general form for combining $n$ multiple phase steps of equal size $\Delta\phi = 2\pi/n$ to isolate the fringing component is

$$\mathbf{W}(\nu) = 1/n \sum_n B_\phi\ e^{i2\pi\theta},\ \text{where } \theta = \phi \tag{5}$$

and the case of four exposures of 90° is

$$\mathbf{W}(\nu) = 1/4[(B_0 - B_{180}) + i(B_{90} - B_{270})]. \tag{6}$$

A whirl can also be called a moiré or beat pattern, and it represents originally high feature frequencies that have been heterodyned (beaten) down to low feature frequencies that more easily survive the blurring of the spectrograph. By combining Eqs. 3, 4 and 6 it can be shown that

$$\mathbf{W}(\nu) = 1/2[S_0(\nu)e^{i2\pi\tau\nu}] \otimes LSF_0(\nu)\ . \tag{7}$$

and the Fourier transform of the whirl is

$$\mathbf{w}(\rho) = (1/2)\gamma\ s_0(\rho + \tau)\ lsf_0(\rho) \tag{8}$$

where we include the interferometer visibility ($\gamma$) previously taken as unity. This important equation describes the EDI formation of moiré fringes on the CCD detector, a heterodyning effect expressed in the $s_0(\rho + \tau)$ argument. Fine spectral details having high feature density $\rho$ are heterodyned (shifted by $\tau$ to the "left") to lower $\rho$ (forming broader features) prior to any blurring by the spectrograph's line spread function. This is the point of view from the CCD detector.

An alternate point of view is from the stellar spectrum. The sensitivity peak of the EDI for detecting the presence of a given $\rho$ in the stellar spectrum has shifted from the origin to the "right", toward higher $\rho$'s. That is,

$$lsf_{edi}(\rho) = (1/2)\gamma\ lsf_0(\rho - \tau). \tag{9}$$

The $lsf_{edi}$ are plotted as the solid curves for $\gamma$=1 in Fig. 5 and 6 where $lsf_0(\rho)$ is modeled as a Gaussian. The conventional sensitivity $lsf_0(\rho)$ are plotted as dashed curves. Below these Figures are plotted the Fourier transform of the derivative of the spectrum, e.g. $\rho\ s(\rho)$, which indicates what $\rho$'s are most important in eliciting a Doppler signal.

### 2.2.1. Conventional spectrum from EDI raw data

Because of the "1" in Eq. 3 the EDI instrument returns both the conventional spectrum and a fringing spectrum from the same data set. In other words, satisfying the rule of conservation of energy, if you sum the two complementary interferometer outputs you get back the input beam (neglecting minor surface losses). The interferometer (Fig. 2) can be thought of as a switching device that sorts photons into two outputs, depending on the detailed wavenumber. Every photon entering the ideal interferometer is passed to the spectrograph.

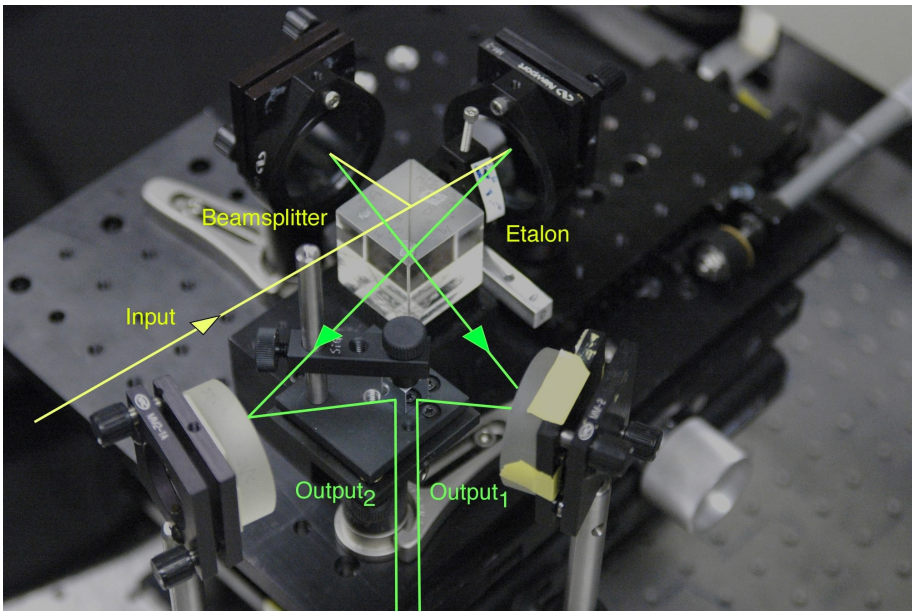


**Figure 2.** Photograph of a dual-output Michelson interferometer. The two outputs differ in phase by 180 degrees, and are directed to different portions of the spectrograph slit so they are recorded by different CCD pixels. The sum of the two outputs equals the input of the interferometer. Hence, by summing these two intensities in the recorded CCD data, the ordinary (nonfringing) spectrum can be obtained. Subtracting the two outputs produces a fringing signal. Thus both fringing and conventional spectral components can be obtained by an EDI from the same CCD data.

The conventional spectrum is obtained by summing the raw EDI phase-stepped data so that fringing terms cancel, such as

$$S_c(\nu) = 1/4(B_0 + B_{180} + B_{90} + B_{270}) \; . \tag{10}$$

Both the conventional and the fringing derived Doppler signals can be used to produce a Doppler velocity signal from an EDI. Because they manifest different spatial frequencies on the CCD detector they are statistically independent and add in quadrature. However, the EDI Doppler signal is dramatically less affected by instrumental errors such as pupil shape change or spectral focal spot drift. Hence if these insults are strong the user may elect to abandon the conventional Doppler signal and use only the EDI Doppler signal.

### 2.2.2. Instrument linespread functions

Figure 3 shows the instrument linespread functions for the conventional and fringing EDI components. They are obtained by running the model with a delta function (impulsive) input spectrum, and are associated with Eqs. 1 and 2 for the conventional, and Eq. 9 or Eqs. 15 to 17 for the EDI. The asterisk in the Figure reminds us that the EDI apparatus produces both conventional (from Eq. 10) and fringing responses (from Eq. 6).

## 2.3. EDI Doppler response

For a nonrelativistic velocity $V$, the wavenumber scales as $\nu \rightarrow (1 + V/c)\,\nu$, so that over a limited bandwidth there appears to be a shift $\Delta\nu_D = (\Delta V/c)\,\nu$. The EDI Doppler measurement uses the change in moiré phase. The moiré pattern is described by the whirl: $\mathbf{W}(\nu) = \frac{1}{2}\left[e^{i2\pi\tau\nu} S_o(\nu)\right] \otimes LSF_0(\nu)$. A Doppler shift causes the whirl to rotate: $\mathbf{W}_1(\nu) = \mathbf{W}_0(\nu)\, e^{-2\pi\tau\Delta\nu}$ by an angle $\tau\Delta\nu_d$. Changing $\tau\Delta v_D$ by unity corresponds to a whirl revolution and the velocity per fringe proportionality (VPF) is $VPF = (\lambda/\tau)c$. The VPF for $\lambda = 1.66\,\mu$m and $\tau = 2$ cm, is ~25,000 m/s per fringe. We make a simultaneous measurement of both the stellar and reference (cell) spectra, and thus the same value of $\tau$ applies to each. Since the Doppler velocity is a difference between those two components, EDI is robust against instrument instabilities causing small drifts in $\tau$.

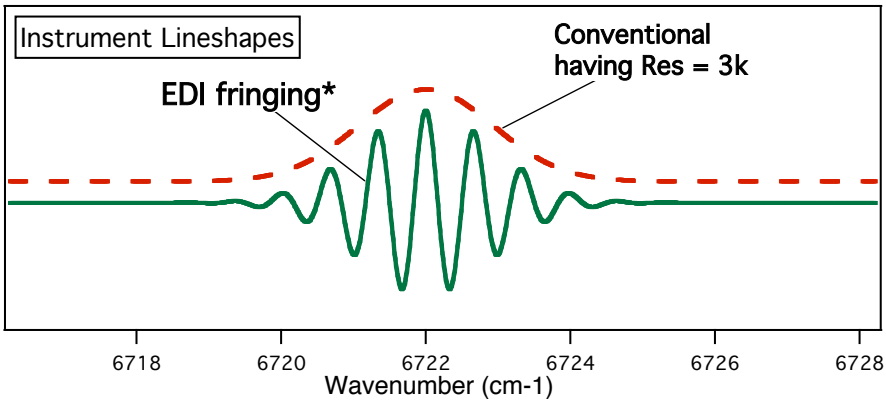


**Figure 3.** Effective instrument linespread functions $LSF(\nu)$ for the conventional (dashed) and fringing portion of EDI (solid), for native disperser resolution Res=3k and delay $\tau$=1.5 cm. (The asterisk reminds us that the EDI apparatus produces both fringing and conventional components, and that the label "EDI" usually refers to the fringing portion.) Note that the period of the oscillation for the EDI linespread is $1/\tau$ or 0.67 cm$^{-1}$, and that its envelope is approximately the conventional linespread. The convolution of these instrument linespreads against the input spectrum $S_0(\nu)$ produces the spectra in Fig. 4

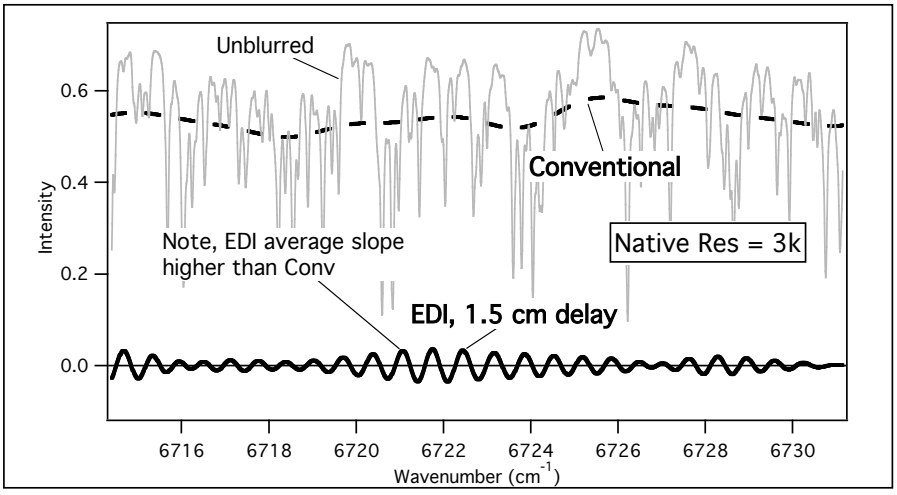


**Figure 4.** Model spectra before [gray, $S_0(\nu)$] and after convolution by instrument linespreads, conventional and EDI. (Instrument linespreads shown in Fig. 3.) The dashed curve $S_c(\nu)$ is the spectrum conventionally blurred by Res=3k. The oscillatory solid curve $S_{edi}(\nu)$ is the effective convolved spectrum of the EDI using delay of 1.5 cm and native spectrograph resolution Res=3k. Because the average value of its slope is greater than that of the conventional spectrum, it has a higher $Q$ and thus produces a greater photon limited Doppler signal to noise ratio.

## 3. DOPPLER QUALITY FACTOR

The radial velocity measurement noise is a function of the characteristic spectral derivative and the number of photons recorded. The photon limited velocity noise ($\delta V$) in a radial velocity measurement is given by Pierre Connes[17]

$$\delta V = \frac{c}{Q}\frac{1}{\sqrt{N}} \tag{11}$$

where $N$ is the total number of detected photons summed over the bandwidth in question. The $Q$ is a dimensionless normalized RMS average of the spectrum's derivative. Therefore, Q is high and the noise is low when the spectral lines are numerous and narrow. The Doppler velocity signal to noise ratio is proportional to $Q$.

For calculating $\delta V$ when $Q(\nu)$ or the intensity $dN/d\nu$ varies with $\nu$, one integrates $Q^2(\nu)dN/d\nu$ over the bandwidth in question, takes the square root, and substitutes that value for $Q\sqrt{N}$ in Eq. 11.

For a conventional spectrograph for photon noise (as opposed to detector noise), $Q$ is given by

$$Q_c^2 = \frac{\langle(\nu^2/S_c)(\partial S_c/\partial\nu)^2\rangle}{\langle S_c\rangle} \tag{12}$$

where $S_c$ is the blurred spectrum Eq. 1. For the EDI,

$$Q_{edi}^2 = \frac{\langle(\nu^2/S_c)|\partial\mathbf{W}'/\partial\nu|^2\rangle}{\langle S_c\rangle}. \tag{13}$$

Due to the heterodyning action, $\mathbf{W}'$ senses the sharp features of the input spectrum before it is blurred by the spectrograph. Hence the derivative $|\partial\mathbf{W}'/\partial\nu|$ can be much higher than for the conventional instrument, generating a higher $Q$.

The $\mathbf{W}'$ and its Fourier transform $\mathbf{w}' = \mathbf{w}(\rho-\tau)$ express the whirl from point of view of the stellar spectrum instead of the CCD detector. That is, where the native spectrograph sensitivity peak has been shifted to the "right"

$$\mathbf{w}' = (1/2)\gamma\ s_0(\rho)\ lsf_0(\rho-\tau) = s_0(\rho)\ lsf_{edi}(\rho). \tag{14}$$

### 3.0.1. EDI expression using purely real spectra

While the natural mathematical space for expressing a fringing spectrum is a complex wave, these are not as intuitive to readers and easily plotted on paper as purely real functions. To provide a more intuitive linkage between EDI and conventional behavior we have developed an alternative and equivalent method for calculating $Q$ that expresses the EDI measured spectra also as purely real spectra $S_{edi}(\nu)$, and from the point of view of the stellar spectrum instead of the CCD detector.

This can be done by using a type of FFT (fast Fourier transform) operation which produces a single-sided spectrum from a purely real function, where the negative frequency branch is assumed to be the complex conjugate of the positive branch, and only the positive branch is shown and manipulated.

Let

$$s_{edi}(\rho) = s_0(\rho)\ lsf_{2,edi}(\rho) \tag{15}$$

where $lsf_{2,edi}(|\rho|)$ differs from the dual-branch $lsf_{edi}(|\rho|)$ of Eq. 9 because it is restricted to positive feature frequencies. We let

$$lsf_{2,edi}(|\rho|) = (1/2)\gamma[lsf_0(\rho-\tau)\ \oplus\ lsf_0(\rho+\tau)] \tag{16}$$

and the "$\oplus$" symbol represents a sum in quadrature. The expression contains two components, with arguments having $\rho+\tau$ and $\rho-\tau$. These come from situations at high resolutions and small $\tau$ when the $lsf_{edi}$ response peak, because it is so wide, extends over both the positive and negative frequency branches. By using the sum in quadrature over both terms we can include signal energy from the negative branch when evaluating only the positive branch.

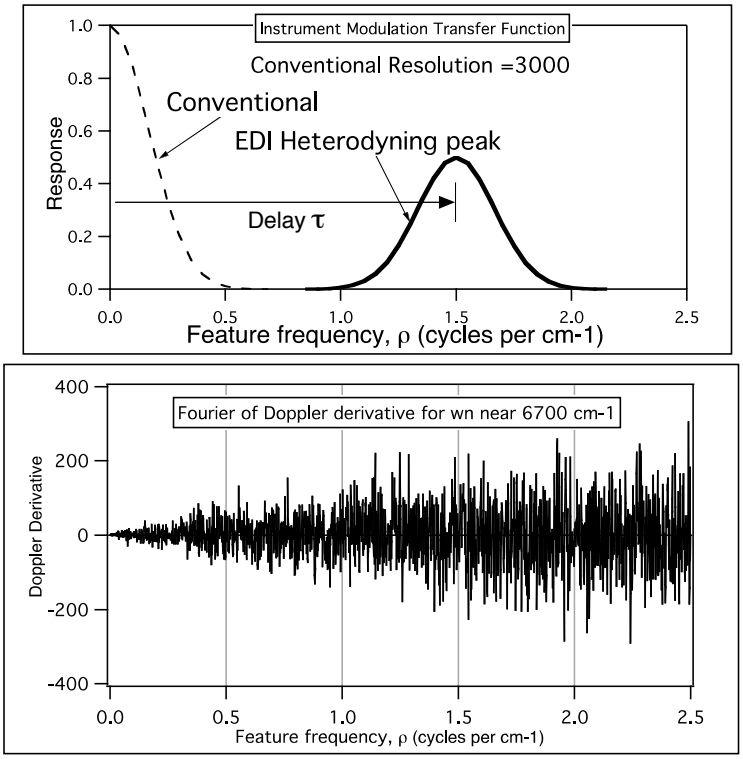


**Figure 5.** (UPPER graph) Modulation transfer function for the EDI instrument having an interferometer delay of 1.5 cm using a spectrograph with a native resolution of Res=3k. Horizontal axis is feature frequency ($\rho$) in stellar spectrum. An EDI produces both conventional (dashed) and a heterodyned (solid) responses. The conventional response is the native spectrograph linespread function $lsf_0(\rho)$, modeled as a Gaussian peak centered at zero $\rho$. It passes only low feature frequencies. The EDI heterodyning response (solid curve) is $lsf_0(\rho)$ shifted by the interferometer delay ($\tau$) and halved in amplitude. It can pass much higher feature frequencies than the conventional response. The user can choose $\tau$ to optimize response based on distribution of Doppler derivative signal (LOWER graph), which is FFT of derivative of the input spectrum. (Here, for the spectrum without rotational blurring, the Doppler derivative continues to grow in strength up to about $\rho$ of 5 cm.)

Next we perform the inverse of the single-sided FFT to obtain the purely real EDI convolved spectrum

$$S_{edi}(\nu) = iFFT\ s_{edi}(\rho) \tag{17}$$

where $S_{edi}(\nu)$ is a real function. This is what is plotted in Fig. 4 along with the conventionally convolved spectrum, and the unblurred spectrum. And in place of the magnitude squared of the derivative in Eq. 13 we use the ordinary square of S

$$\langle|\partial \mathbf{W}'/\partial\nu|^2\rangle = \langle(\partial S_{edi}/\partial\nu)^2\rangle. \tag{18}$$

### 3.0.2. EDI calculation of Q without invoking heterodyning

A third and independent method of calculating EDI $Q$ is called the Doppler reaction function approach. It operates in the CCD detector space instead of the stellar spectrum space. It simulates the change in the CCD detector signal when the wavenumber position of an absorption spectrum is translated by a given amount, such as due to a Doppler shift. The input spectrum is multiplied by a sinusoidal comb and blurred (following Eq. 4). It does not invoke any heterodyning process, and does not require any Fourier transform, and operates with purely real functions. This Doppler reaction method has been previously described in more detail in Ref. 5 for the example of a single Gaussian absorption line. We have verified that all three methods give the same result for $Q$.

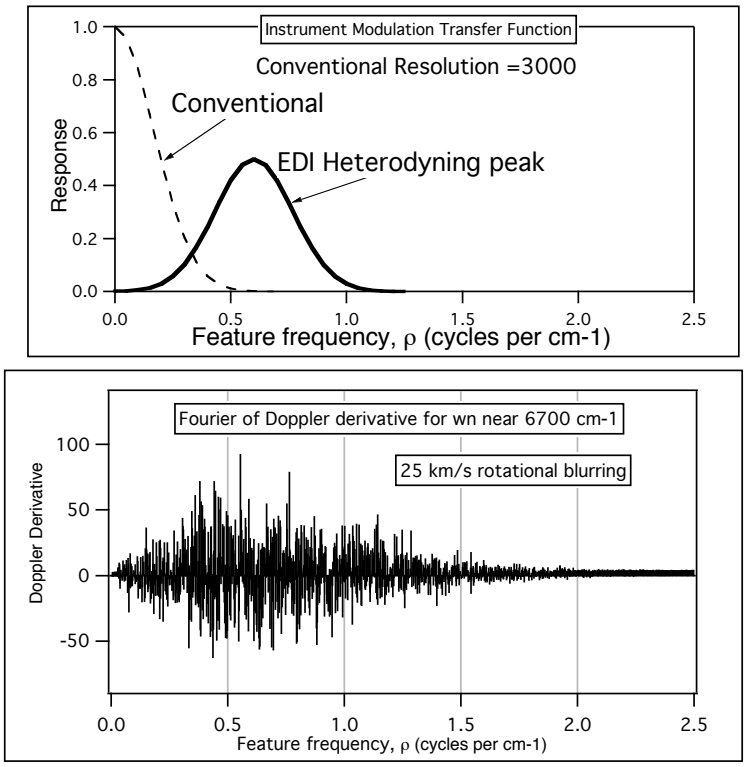


**Figure 6.** Same as Fig. 5 but with 25 km/s rotational blurring and $\tau$=0.6 cm. The rotation kills off high feature frequencies in the Doppler derivative (lower graph), hence $\tau$ is reduced to 0.6 cm to slide the heterodyning peak over location of maximum Doppler signal energy, to optimize $Q$.

## 4. RESULTS

### 4.1. Q results

Figure 7 shows the calculated Q versus wavenumber for a stellar model[16] having temperature 1600K, gravity g=1000, and no rotational blurring. The Q varies about an order of magnitude from one region to another. High Q regions tend to be also where the telluric lines are dense, which reduces the local flux and makes it more difficult to separate telluric lines from stellar lines.

The $Q$ for the EDI (solid curve) using an interferometer delay $\tau$=1.5 cm is about 6 times greater than the $Q$ for conventional instrument, and 8 times for $\tau$=5 cm, because the EDI is sensitive to narrower spectral features. The dependence of the $Q$ spectrum on simple rotational blurring is shown in Figure 8, for speeds 7.5, 15, and 25 km/s, and $\tau$ of 0.6, 0.9, 1.5 and 5 cm, simulated by pre-blurring the stellar spectrum with a Gaussian blur. For example since $3 \times 10^8/7500 = 40$k, a Gaussian blur of Res=40k was applied for the 7.5 km/s case, prior to the convolutions with the instrument linespreads. As the rotational blur increases, the interferometer delay was decreased from 5 cm to 0.6 cm to roughly follow the maximum in the Doppler derivative FFT, as shown in lower graph of Fig. 6.

### 4.2. Shape of spectra and linespread function

The effect of the instrument on the input spectrum, which is the stellar model with no rotational blurring, is shown in Fig. 4. The original high resolution spectrum $S_0(\nu)$ is shown in gray. The conventional spectrum $S_c(\nu)$ convolved with an ordinary Gaussian instrument lineshape of resolving power 3k [defined by the FWHM of $LSF_0(\nu)$] is shown as the dashed curve. The high resolution features that would produce a significant Doppler

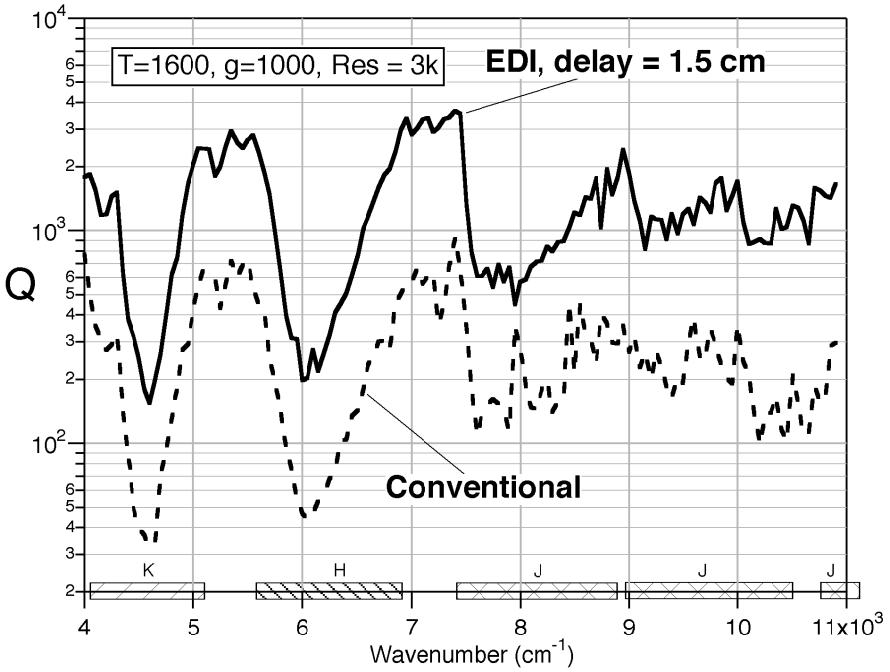


**Figure 7.** A spectrum's Doppler quality ($Q$) versus wavenumber ($\nu$), calculated for a stellar model having temperature T=1600, gravity g=1000, and no rotational blurring. The Doppler velocity signal to noise ratio is proportional to $Q$. Model spectrum[16] from D. Saumon, M. Marley and R. Freedman. Shown are conventional $Q$ and EDI $Q$ for native spectrograph resolution Res=3k and interferometer delay of 1.5 cm. Even higher $Q$ is obtained at delay of 5 cm (see Fig. 8). Band labels at bottom avoid major telluric line regions.

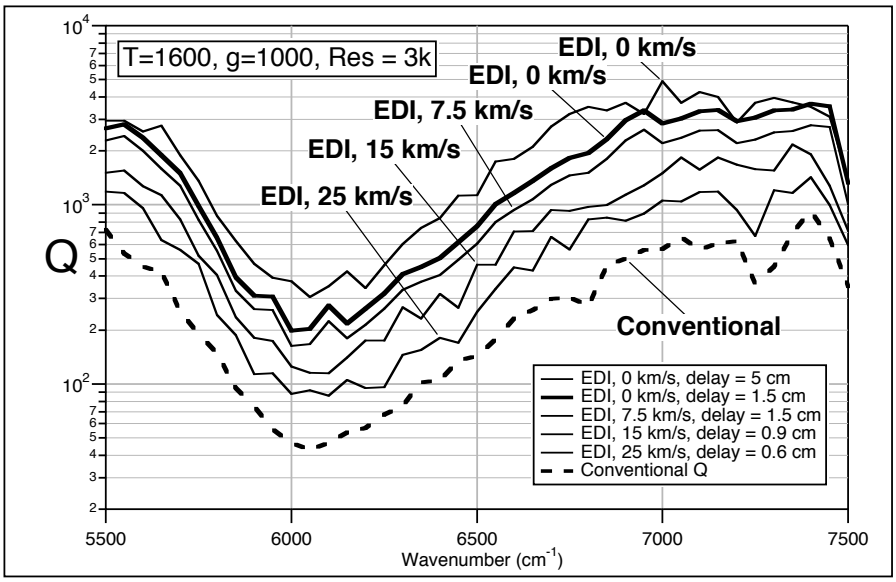


**Figure 8.** Effect of stellar rotation on $Q$ for 0, 7.5, 15, and 25 km/s and various delays from 0.6 to 5 cm. The input spectrum was Gaussian blurred to simulate approximate rotational blurring and used instead of the input spectrum. For the 3k spectrograph resolution used here the conventional $Q$ did not vary significantly with rotational speed, and only the zero velocity conventional result was shown (dashed).

sensitivity are obliterated by the conventional blurring. Hence using a Res=3k instrument in the conventional manner for Doppler velocimetry would produce inferior results.

The analogous EDI convolved spectrum $S_{edi}(\nu)$ is shown as the solid oscillatory curve. This uses the same native spectrograph resolution of Res=3k and with an interferometer delay of $\tau$=1.5 cm. This is a convolution of the gray curve with the EDI linespread function shown in Fig. 3 using Eqs. 15 to 17. The linespread functions of Fig. 3 are obtained by running the model with a delta function (impulse) input spectrum.

#### 4.2.1. Display in Fourier domain

While displaying the instrument response *LSF* in the familiar dispersive ($\nu$) space is intuitive, it is more useful for choosing the optimum interferometer delay value $\tau$ to show the instrument response *lsf* in $\rho$ space, which is the Fourier transform of the dispersive space, which is a modulation transfer function. This is done in the upper graphs of Fig. 5 and 6. The conventional response is the dashed Gaussian at the origin, and the EDI response is the solid curve, which is the same shape Gaussian as the conventional response but translated to the right by amount $\tau$ and halved in amplitude. This shows that the EDI is much more sensitive to high feature frequencies than the conventional spectrograph without the interferometer. These high feature frequencies contain the majority of the Doppler strength of the stellar spectrum, as shown in the lower graphs.

The lower graphs of Fig. 5 and 6 show the distribution of Doppler strength among $\rho$. These are the Fourier transform of the derivative of the input spectrum (after any rotational blurring, but before instrument blurring), given by $\rho\, s_0(\rho)$. It is optimal to choose $\tau$ to place the heterodyning peak (solid curve) at the maximum strength of the Doppler derivative. This location moves to the left (starting from about 5 cm) with increasing rotational blurring– at about 25 km/s the maximum is at about 0.6 cm as seen in Fig. 6.

## 5. CONCLUSION

The EDI will return a higher $Q$, and thus a better photon-limited Doppler velocity signal to noise ratio than the conventional instrument, which is a dispersive spectrograph used without an interferometer. The improvement is most dramatic for low native spectrograph resolutions and stellar spectra having a large amount of high resolution features. Large amounts of rotational blurring will reduce the advantage.

However, even under extreme rotational blurring, an ideal throughput (i.e. using both outputs) EDI instrument will retain an advantage because its Doppler velocity result can be combined with the conventional Doppler velocity result that comes for free from the same set of exposures. The net $Q$ would be the sum in quadrature of $Q_{edi}$ and $Q_c$. Hence the net Doppler signal to noise ratio will be better with the interferometer than the grating used alone. In other papers (see Fig. 10 of Ref. 10) we have described how the EDI Doppler velocity result is much more robust to instrumental drifts, such as pupil and spectrograph focal spot size and position changes. Frequently these are more important than the photon noise in limiting performance. Hence, even under extreme rotational blurring the EDI is advantageous in extracting the most favorable Doppler signal from a grating spectrograph.

(Fundamentally, the robustness to environmental insults is because the EDI measures a differential effect: the moiré pattern created in the spectra, which are beats between the science spectrum and the sinusoidal interferometer transmission. The science signal and the sinusoidal peaks and valleys are married together and suffer the same distortions as they pass through the spectrograph optics. Hence the phase of the moiré pattern can be several orders of magnitude less sensitive to focal spot changes. This allows an inexpensive spectrograph to perform precision Doppler velocities when otherwise impractical due to lack of environmental controls or heavy sturdy optical mounts.)

## ACKNOWLEDGMENTS

Thanks to Didier Saumon, Mark Marley, Richard S. Freedman and Travis Barman for high resolution stellar models. This work was performed with support from the National Science Foundation (awards AST-0504874 & AST-0505366), and under the auspices of the U.S. Department of Energy by the University of California, Lawrence Livermore National Laboratory under contract No. W-7405-Eng-48.

## REFERENCES


1. D. Erskine, "Single and Double Superimposing Interferometer Systems," *US Patent* **6,115,121**, Issued Sept. 5, 2000.
2. D. Erskine, "Combined Dispersive/Interference Spectroscopy for Producing a Vector Spectrum," *US Patent* **6,351,307**, Issued Feb. 26, 2002.
3. D. Erskine and J. Ge, "Novel Interferometer Spectrometer for Sensitive Stellar Radial Velocimetry," in *Imaging the Universe in Three Dimensions: Astrophysics with Advanced Multi-Wavelength Imaging Devices*, W. van Breugel and J. Bland-Hawthorn, eds., *ASP* **195**, p. 501, 2000.
4. J. Ge, D. Erskine, and M. Rushford, "An Externally Dispersed Interferometer for Sensitive Doppler Extrasolar Planet Searches," *PASP* **114**, pp. 1016–1028, 2002.
5. D. Erskine, "An Externally Dispersed Interferometer Prototype for Sensitive Radial Velocimetry: Theory and Demonstration on Sunlight," *PASP* **115**, pp. 255–269, 2003.
6. J. Ge, "Fixed Delay Interferometry for Doppler Extrasolar Planet Detection," *ApJ* **571**, pp. L165–168, 2002.
7. J. Ge, "Erratum: Fixed Delay Interferometry for Doppler Extrasolar Planet Detection," *ApJ* **593**, p. L147, 2003.
8. D. Erskine, J. Edelstein, M. Feuerstein, and B. Welsh, "High Resolution Broadband Spectroscopy using an Externally Dispersed Interferometer," *ApJ* **592**, pp. L103–L106, 2003.
9. D. J. Erskine and J. Edelstein, "Interferometric Resolution Boosting for Spectrographs," in *Ground-based Instrumentation for Astronomy. Edited by Alan F. M. Moorwood and Iye Masanori. Proceedings of the SPIE, Volume 5492, pp. 190-199 (2004).*, pp. 190–199, Sept. 2004.
10. D. Erskine and J. Edelstein, "High-resolution Broadband Spectral Interferometry," in *Future EUV/UV and Visible Space Astrophysics Missions and Instrumentation, ed. J. C. Blades, O. H. Siegmund*, pp. 158–169, SPIE Proc. 4854, Feb. 2003.
11. J. Edelstein and D. Erskine, "High Resolution Absorption Spectroscopy using Externally Dispersed Interferometry," in *UV, X-ray & Gamma Ray Astr. Space Instrm.*, SPIE Proc. 5898, August 2005.
12. D. Erskine, J. Edelstein, D. Harbeck, and J. Lloyd, "Externally Dispersed Interferometry for Planetary Studies," in *Techniq. & Instrm. for Detect. Exo-planets*, SPIE Proc. 5905, August 2005.
13. J. C. van Eyken, J. Ge, S. Mahadevan, and C. DeWitt, "First Planet Confirmation with a Dispersed Fixed-Delay Interferometer," *ApJ* **600**, pp. L79–L82, Jan. 2004.
14. J. Ge, J. van Eyken, S. Mahadevan, C. DeWitt, S. Kane, R. Cohen, A. Vanden Heuvel, S. Fleming, P. Guo, G. Henry, D. Schneider, L. Ramsey, R. Wittenmyer, M. Endl, W. Cochran, E. Ford, E. Martin, G. Israelian, J. Valenti, and D. Montes, "The First Extrasolar Planet Discovered with A New Generation High Throughput Doppler Instrument," *ApJ* **accepted**, 2006.
15. J. C. Wilson, C. P. Henderson, T. L. Herter, K. Matthews, M. F. Skrutskie, J. D. Adams, D.-S. Moon, R. Smith, N. Gautier, M. Ressler, B. T. Soifer, S. Lin, J. Howard, J. LaMarr, T. M. Stolberg, and J. Zink, "Mass producing an efficient NIR spectrograph," in *Ground-based Instrumentation for Astronomy. Edited by Alan F. M. Moorwood and Iye Masanori. Proceedings of the SPIE, Volume 5492, pp. 1295-1305 (2004).*, A. F. M. Moorwood and M. Iye, eds., pp. 1295–1305, Sept. 2004.
16. D. Saumon, 2006. Los Alamos Nat. Lab., personal communication.
17. P. Connes, "Absolute Astronomical Accelerometry," *Astrph. & Spc. Sci.* **110**, p. 211, 1985.